Chemical Engineering and Processing 70 (2013) 27–36

Contents lists available at SciVerse ScienceDirect

Chemical Engineering and Processing: Process Intensification

journal homepage: www.elsevier.com/locate/cep

An investigation in the effects of recycles on laminar heat transfer enhancement of parallel-flow heat exchangers

Yonghua You[a,b], Aiwu Fan[a,*], Xiaojun Luo[a], Shiping Jin[a], Wei Liu[a], Suyi Huang[a]

[a] School of Energy and Power Engineering, Huazhong University of Science and Technology, Wuhan 430074, China
[b] School of Materials and Metallurgy, Wuhan University of Science and Technology, Wuhan 430081, China

ARTICLE INFO

Article history:
Received 7 March 2013
Received in revised form 10 May 2013
Accepted 13 May 2013
Available online 29 May 2013

Keywords:
Laminar flow
Heat transfer
Mathematical model
Numerical analysis
Heat exchanger
Internal/external recycle

ABSTRACT

It was demonstrated that fluid recycling could effectively enhance heat transfer rates of heat exchangers, however, related investigations were limited. In the current work, parallel-flow heat exchangers with basic recycles or revised recycles are investigated in the laminar regime. Theoretical models of thermo-hydraulic performances are established. The effects of reflux ratio, capacitance rate ratio, heat transfer area, and recycle length are investigated. The results demonstrate that the dimensionless heat transfer rate rises with the increase of reflux ratio or capacitance rate ratio, or with the decrease of heat transfer area, and the maximum values reach up to 127% and 121% for basic internal and external recycles, respectively. Basic internal recycles generate larger dimensionless heat transfer rates under larger reflux ratios, while basic external recycles perform more reliably over the whole reflux ratio range. Compared with basic recycles, revised recycles (i.e., partial-length recycles) require smaller pumping powers. Thus, partial-length recycles can improve the dimensionless overall performance of full-length recycle heat exchangers, e.g., half-length recycles increase the dimensionless overall performance by 65%. Fluid recycling does not need to change geometrical structures and fluid flow rates, thus it is a competitive approach of thermal augmentation in heat exchangers.

1. Introduction

Heat transfer between hot and cool fluids separated by a solid wall is a common and important process in a variety of industrial fields, such as power generation, petroleum refining and chemical processes, etc. [1]. To improve the thermal efficiency, heat transfer enhancement has been hotly investigated for decades. Extended surfaces and disturbance elements are two of the most widely applied techniques of thermal augmentation. In the former technique, ribs or fins are attached to passage walls to increase the heat transfer area [2–4]. Meanwhile, ribs generate periodical vortexes which can disturb the thermal boundary layer. Thus, high heat transfer rate can be obtained. Disturbance elements could be divided into two categories. One is the tube insert, such as twisted tapes [5,6], wire coils [7], and strip inserts [8–10]; the other includes various tube-bundle support structures, to name a few, segmental baffles [11,12], rod baffles [13], helical baffles [14], flower baffles [15,16] and trefoil-hole baffles [17], etc. Although the disturbance elements cannot increase heat transfer area, they exert intensive disturbances and induce fluid to wash heat transfer surfaces. Therefore, the bulk temperature becomes more uniform and the thickness of thermal boundary layer is decreased. As a result, the heat transfer rate is effectively enhanced due to these elements.

In addition to the above-mentioned techniques, utilization of recycles was proposed by scholars for the heat transfer argumentation [18], and several theoretical and experimental researches were conducted to investigate the effects of recycles. Ho et al. [19] solved the 2-D differential conservation equations of laminar heat transfer in a parallel-plate channel with an external recycle. The analytical solution under uniform wall temperature conditions agreed qualitatively with experimental data. Yeh and Ho [20] and Yeh et al. [21] researched the effects of external recycles on solar air heaters without or with internal fins, respectively. The former investigation based on 1-D model demonstrated that an improvement over 80% in collector efficiency is available. In addition, Yeh [22] investigated the heat transfer enhancement with external recycles in parallel-flow heat exchangers. He obtained the distributions of fluid temperatures via introducing the parameters of dimensionless fluid temperatures, and found that considerable improvement of heat transfer rate could be achievable.

* Corresponding author at: School of Energy and Power Engineering, Huazhong University of Science and Technology, 1037 Luoyu Road, Wuhan 430074, China. Tel.: +86 27 87542618; fax: +86 27 87540724.
E-mail addresses: faw@hust.edu.cn, catia315@163.com, faw@mail.hust.edu.cn (A. Fan).

0255-2701/$ – see front matter © 2013 Elsevier B.V. All rights reserved.
http://dx.doi.org/10.1016/j.cep.2013.05.010

Nomenclature

A	heat transfer area (m^2)
c_p	specific heat of constant pressure (J/(kg K))
C	capacitance rate (W/K)
C_R	the minimum of capacitance rate ratio
D	characteristic length (m)
h	surface heat transfer coefficient (W/(m^{2}K))
H	passage height (m)
L	passage length (m)
K	overall heat transfer coefficient (W/(m^2 K))
NTU	number of heat transfer unit
Δp	pressure loss (Pa)
P	pumping power (W)
q_V	volumetric flow rate (m^3/s)
Q	heat transfer rate (W)
R	reflux ratio
Re	Reynolds number
t	temperature (K)
Δt	heat transfer difference (K)
W	passage width (m)
ρ	fluid density (kg/m^3)
μ	dynamic viscosity (kg/(m s))
λ	thermal conductivity (W/(m K))
η	effectiveness of heat exchanger

Superscripts

in	inlet
out	outlet
a, *b*, *c*, *d*, *e*	positions of passage

Subscripts

1	hot fluid side; recycle
2	cool fluid side
b	bottom module of HE-BIR
BER	with a basic external recycle
BIR	with a basic internal recycle
c	core part of HE-BER
l	left module of HE-RER or HE-RIR
m	mean
NR	no recycle
r	right module of HE-RER or HE-RIR
RER	with a revised external recycle
RIR	with a revised internal recycle
t	total
u	upper module of HE-BIR

It is clear that the investigation in heat transfer enhancement with recycles is inadequate, for all the above-mentioned investigations focused on the effects of external recycles, and the effects of geometrical parameters (e.g., heat transfer area) have not been studied either. The internal recycle is another typical recycle arrangement, which is expected to have different characteristics compared with the external recycle. However, to the best of our knowledge, no related investigation has been published heretofore. Therefore, in the current work, basic external and internal recycles, as well as revised recycles (i.e., partial-length recycles), are studied to improve the performances of parallel-flow heat exchangers. The mathematical models of thermo-hydraulic performances of these recycle heat exchangers are constructed based on the counterparts of ordinary heat exchangers (i.e., with no recycle), and special attentions are paid to the effects of both working conditions and geometrical parameters, such as the reflux ratio, capacitance rate ratio, heat transfer area and recycle length.

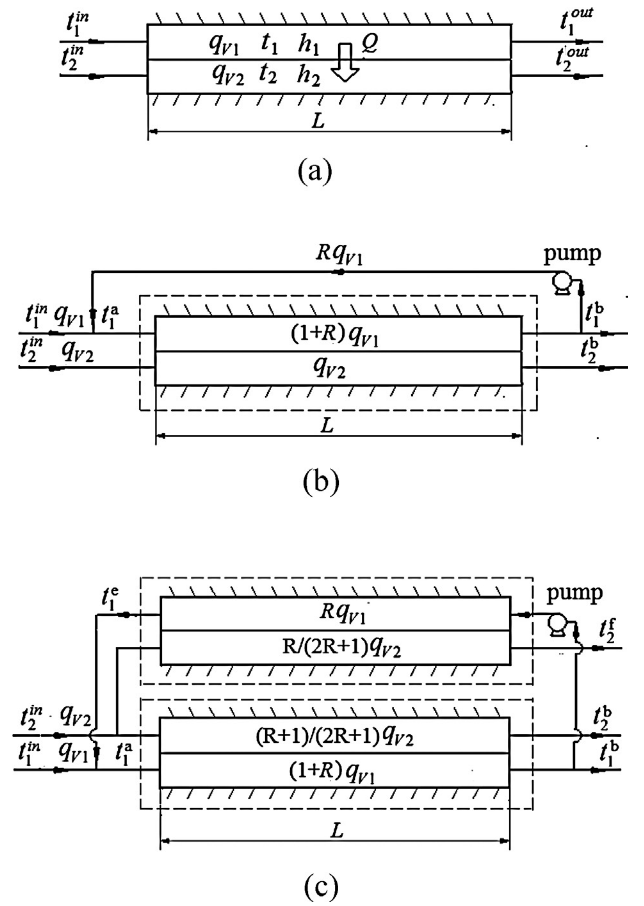

Fig. 1. Schematics of HE-NR, HE-BER and HE-BIR. (a) HE-NR; (b) HE-BER; and (c) HE-BIR.

2. Theoretical model of thermo-hydraulic performance

2.1. Derivation of heat transfer rate and averaged heat transfer temperature difference

2.1.1. Parallel-flow heat exchanger without recycle

Fig. 1a depicts a heat exchanger with no recycle (HE-NR) working under the cocurrent flow condition. The hot and cooling fluids, whose parameters are marked by subscripts 1 and 2, respectively, flow parallel to each other in the adjacent passages, and exchange heat through a solid wall. Since the outside walls of heat exchanger are insulated, the enthalpy increment of cool fluid equals to the enthalpy decrease of hot fluid, and also equals to the heat flow through the solid wall. With the above energy conservations, the differential temperature difference between hot and cool fluids can be expressed by the temperature difference of their own, as shown in Eq. (1) [23].

$$d(t_1 - t_2) = -\frac{1}{\rho_1 q_{V1} c_{p1}} \left(1 + \frac{\rho_1 q_{V1} c_{p1}}{\rho_2 q_{V2} c_{p2}}\right) dQ = -\left(1 + \frac{C_1}{C_2}\right) \frac{K(t_1 - t_2)}{C_1} dS \quad (1)$$

where t and Q refer to the bulk temperature of fluid and heat flow through the solid wall. C stands for the capacitance rate of fluid, calculated by $C = \rho q_V c_p$. K represents the overall heat transfer coefficient from the hot fluid to cool fluid.

With the assumption that both hot and cool fluids have constant properties, and the value of K is uniform along the passage, the averaged heat transfer temperature difference of HE-NR under the cocurrent flow condition can be derived from the integration of Eq. (1), as shown in Eq. (2) [23].

$$\Delta t_m = \frac{Q}{KA} = (t_1^{in} - t_2^{in})\frac{1-\exp(-(1+C_R)\mathrm{NTU})}{(1+C_R)\mathrm{NTU}} \tag{2}$$

where A and t^{in} stand for the heat transfer area and incoming temperatures of working fluids, respectively. C_R represents the minimum of capacitance rate ratio between the hot and cool fluids, i.e., $C_R = \min(C_1/C_2, C_2/C_1)$, while NTU stands for the number of transfer units, calculated by $\mathrm{NTU} = KA/\min(C_1, C_2)$ [23].

If we reverse the flow direction of cool fluid, the HE-NR of Fig. 1a works under the countercurrent condition (the schematic is not given here), and the averaged heat transfer temperature difference is calculated through Eq. (3) [23].

$$\Delta t_m = \frac{Q}{KA} = (t_1^{in} - t_2^{in})\frac{1-\exp(-\mathrm{NTU}(1-C_R))}{((1-C_R\exp(-\mathrm{NTU}(1-C_R)))\mathrm{NTU}} \tag{3}$$

Effectiveness of heat exchanger, i.e., the ratio between actual heat transfer rate of the heat exchanger and maximum possible heat transfer rate under the identical inlet conditions, is expressed by Eq. (4) [23].

$$\eta = \max\left(1, \frac{C_1}{C_2}\right)\frac{t_1^{in} - t_1^{out}}{t_1^{in} - t_2^{in}} \tag{4}$$

where t^{out} refers to the discharge temperature of working fluid.

Combining Eqs. (2) and (3) with Eq. (4), as well as $\mathrm{NTU} = KA/\min(C_1, C_2)$, we obtain the formulae for the effectiveness of HE-NR under the cocurrent and countercurrent conditions, as shown in Eqs. (5) and (6), respectively.

$$\eta = \frac{1-\exp(-(1+C_R)\mathrm{NTU})}{1+C_R} \tag{5}$$

$$\eta = \frac{1-\exp(-\mathrm{NTU}(1-C_R))}{1-C_R\exp(-\mathrm{NTU}(1-C_R))} \tag{6}$$

The heat transfer rate through solid wall can be calculated with the averaged heat transfer temperature difference, or the effectiveness of heat exchanger, as shown in Eq. (7) [23].

$$Q = KA\Delta t_m = \frac{\eta C_1(t_1^{in} - t_2^{in})}{\max(1, C_1/C_2)} \tag{7}$$

2.1.2. Parallel-flow heat exchanger with a basic external recycle

The heat exchanger with a basic external recycle (HE-BER) is schematically depicted in Fig. 1b, in which a part of cooled hot fluid is delivered by a pump to the inlet port and mixed with incoming hot fluid for larger convective heat transfer coefficient.

Since the mixing process takes place adiabatically, the inlet temperature of hot fluid, i.e., t_1^a in Fig. 1b, can be obtained from Eq. (8).

$$t_1^a = \frac{t_1^{in} + R\cdot t_1^b}{R+1} \tag{8}$$

where R refers to the ratio between the reflux and incoming flow rate, t_1^{in} and t_1^b represent the incoming and discharge temperatures on the hot fluid side, respectively.

The core of HE-BER, i.e., the part enclosed in the dashed rectangle of Fig. 1b, is a parallel-flow HE-NR. Resulting from the reflux, the capacitance rate of the core part becomes $(1+R)$ times that of incoming fluid on the hot fluid side, and its effectiveness can be expressed by Eq. (9). One can refer to Eqs. (5) and (6) for the effectiveness of HE-BER core under cocurrent and countercurrent flow conditions.

$$\eta_c = \max\left(1, \frac{(R+1)C_1}{C_2}\right)\frac{t_1^a - t_1^b}{t_1^a - t_2^{in}} \tag{9}$$

The definition of total effectiveness of HE-BER is based on the incoming temperatures of the hot and cool fluids. With the combination of Eqs. (8) and (9), the total effectiveness can be calculated based on the core effectiveness, as shown in Eq. (10).

$$\eta_t = \max\left(1, \frac{C_1}{C_2}\right)\frac{t_1^{in} - t_1^b}{t_1^{in} - t_2^{in}} = \max\left(1, \frac{C_1}{C_2}\right)\frac{\eta_c(R+1)}{R\eta_c + \max(1, (1+R)C_1/C_2)} \tag{10}$$

Once the total effectiveness has been obtained, the heat transfer rate and averaged heat transfer temperature difference of HE-BER can be calculated through Eq. (7), where K takes its value when the hot fluid flow rate is $(1+R)q_{V1}$.

2.1.3. Parallel-flow heat exchanger with a basic internal recycle

Similar to a HE-BER, a heat exchanger with a basic internal recycle (HE-BIR) pumps some cooled hot fluid back to the inlet port for larger heat transfer coefficient. Moreover, it simultaneously allocates some heat transfer surfaces and cooling fluid to further chill the recycled hot fluid, as depicted in Fig. 1c. It is seen from Fig. 1c that the whole HE-BIR can be divided into two smaller modules, which are enclosed by two dashed rectangles. The upper module is used to further chill the recycled hot fluid, while the bulk of hot fluid is cooled in the bottom one.

For the convenience of comparison, it is assumed that the total flow rate and flow area of HE-BIR are identical to the counterparts of referred HE-NR. Moreover, to ensure that the flow velocity are uniform between the upper and bottom modules of HE-BIR on both the hot and cool fluid sides, respectively, the ratio of flow area between the two modules are set as $R/(R+1)$, and the allocation of cooling fluid between the two modules takes the same ratio. With the above arrangements, the effectiveness of the upper and bottom modules of HE-BIR take the expressions of Eqs. (11) and (12), respectively, and their values under the cocurrent and countercurrent flow conditions can be derived from Eqs. (5) and (6), respectively.

$$\eta_u = \max\left(1, \frac{(2R+1)C_1}{C_2}\right)\frac{t_1^b - t_1^e}{t_1^b - t_2^{in}} \tag{11}$$

$$\eta_b = \max\left(1, \frac{(2R+1)C_1}{C_2}\right)\frac{t_1^a - t_1^b}{t_1^a - t_2^{in}} \tag{12}$$

where t_1^b refers to the discharge temperature of bottom module, as well as the inlet temperature of upper module on the hot fluid side, while t_1^e represents the discharge temperature of upper module.

As mentioned above, the mixture at the inlet port is an adiabatic process, thus, t_1^a is coupled with t_1^{in} and t_1^e, as shown in Eq. (13).

$$t_1^a = \frac{t_1^{in} + R\cdot t_1^e}{R+1} \tag{13}$$

The total effectiveness of HE-BIR, which is based on the incoming temperatures on the hot and cool fluid sides, can be derived from the combination of Eqs. (11)–(13), as shown in Eq. (14).

$$\eta_t = \max\left(1, \frac{C_1}{C_2}\right)\frac{t_1^{in} - t_1^b}{t_1^{in} - t_2^{in}} = \frac{\max\left(1, C_1/C_2\right) + \max\left(1, C_1/C_2\right)}{((R\eta_b + \max(1, (2R+1)C_1/C_2))/(\eta_b - \max(1, (2R+1)C_1/C_2))) - (R\eta_u/(\max(1, (2R+1)C_1/C_2))} \tag{14}$$

Combining Eqs. (7) and (14), one can derive the heat flow through solid wall and averaged heat transfer temperature difference of HE-BIRs.

2.1.4. Parallel-flow heat exchanger with a revised recycle

Fig. 2a presents a revised external recycle heat exchanger (HE-RER), while a heat exchanger with a revised internal recycle (HE-RIR) is depicted in Fig. 2b. It is seen from Fig. 2 that both heat exchangers employ a pump to draw a part of incompletely cooled hot fluid to the inlet ports and blend with the incoming hot fluids. They can both be divided into two smaller heat exchangers connected in series, as shown in the dashed rectangles of Fig. 2. The right one is a smaller HE-NR with a passage length of L–L_1, while the left one is a smaller HE-BER or HE-BIR with a passage length of L_1. The effectivenesses of the left and right small heat exchangers, i.e., η_l and η_r, are generally expressed by Eqs. (15) and (16), respectively. η_r is the calculated through Eqs. (5) and (6) for cocurrent and countercurrent flow conditions, respectively, while Eqs. (10) and (14) are adopted for the calculations of effectivenesses of smaller HE-BER and HE-BIR, respectively.

$$\eta_l = \max\left(1, \frac{C_1}{C_2}\right)\frac{t_1^{\text{in}} - t_1^b}{t_1^{\text{in}} - t_2^{\text{in}}} \tag{15}$$

$$\eta_r = \max\left(1, \frac{C_1}{C_2}\right)\frac{t_1^b - t_1^d}{t_1^b - t_2^b} \tag{16}$$

With the combination of Eqs. (15) and (16), we found that both the total effectivenesses of HE-RER and HE-RIR can be calculated through Eq. (17), and thus their heat transfer rates can be obtained from Eq. (7).

$$\eta_t = \max\left(1, \frac{C_1}{C_2}\right)\frac{t_1^{\text{in}} - t_1^d}{t_1^{\text{in}} - t_2^{\text{in}}} = \eta_l + \eta_r - \frac{\eta_l\eta_r}{\max(1, C_1/C_2)}\left(1, \frac{C_1}{C_2}\right) \tag{17}$$

2.2. Derivation of overall heat transfer coefficient K

The solid walls of heat exchangers, adopted to separate the hot and cool fluids, are usually manufactured with thin metal plates. Thus, the thermal resistance inside the walls is trivial. When the effects of fouling on heat transfer can be neglected, K is calculated through Eq. (18) [23].

$$K = \frac{h_1 h_2}{h_1 + h_2} \tag{18}$$

where h_1 and h_2 stand for the surface heat transfer coefficients on the hot and cool fluid sides, calculated by the empirical relation of Sieder-Tate, i.e., Eq. (19), for the laminar forced convection [24].

$$h = \frac{1.86\lambda}{D}\left(\text{Re}Pr\frac{D}{L}\right)^{1/3}\left(\frac{\mu_b}{\mu_w}\right)^{0.14} \tag{19}$$

Here, λ and μ stand for heat conductivity and dynamic viscosity of fluid, respectively; L refers to passage length; D is the characteristic dimension and it equals to $2H$ in the present study, because it is assumed that the width (W) of the passages is much larger than the height (H). Re represents the Reynolds number calculated through Eq. (20), in which ρ and q_V stand for the fluid density and volumetric flow rate, respectively.

$$Re = \frac{2\rho q_V}{\mu W} \tag{20}$$

In the core part of HE-BER (see the dashed rectangle of Fig. 1b), the flow rate of hot fluid is increased by R times compared with its referred HE-NR, whose total heat transfer area and flow rate of cooling fluid are the same as the counterparts of the heat exchanger with a recycle. As the flows on the hot and cool fluid sides are in laminar regime in the current investigation, the surface heat transfer coefficient on the hot fluid side becomes $(1 + R)^{1/3}$ times that without recycles according to the empirical relation of Eq. (19). When the working fluids and geometrical parameters on the hot and cool sides are the same, the ratios of K between HE-BERs and referred HE-NRs can be calculated by Eq. (21).

$$\frac{K_{\text{BER}}}{K_{\text{NR}}} = \frac{1 + (C_2/C_1)^{1/3}}{1 + (C_2/((R+1)C_1))^{1/3}} \tag{21}$$

where K_{BER} and K_{NR} stand for the overall heat transfer coefficient of HE-BERs and corresponding HE-NRs, respectively.

A HE-BIR (see Fig. 1c) accommodates the flow rate of hot fluid $(1 + 2R)$ times that without recycle, thus its overall heat transfer coefficient in the laminar flow regime can be obtained by Eq. (22), where the hot and cool fluid sides have the same working fluids and geometrical parameters.

$$\frac{K_{\text{BIR}}}{K_{\text{NR}}} = \frac{1 + (C_2/C_1)^{1/3}}{1 + (C_2/((2R+1)C_1))^{1/3}} \tag{22}$$

As mentioned above, a HE-RER or HE-RIR can be divided into a small HE-NR (channel length L–L_1) and a small HE-BER or HE-BIR (channel length L_1). The overall heat transfer coefficient of the small HE-NR can be calculated through Eq. (18), while Eqs. (21) and (22) are adopted for the calculations of small HE-BER and HE-BIR, respectively, in which the referred HE-NR has the same channel length as the small BER or BIR, i.e., L_1.

2.3. Derivation of pumping power consumption

Since the flows on the hot and cool fluid sides are in the laminar region, the pressure loss is calculated through Eq. (23) [22].

$$\Delta p = \frac{12\mu L \times (\text{volume flow rate})}{H^2 \times (\text{cross-section area})} \tag{23}$$

The pumping powers required for the hot and cool fluids both equal to the products of pressure losses and volumetric flow rates, and the total pumping power requirement is calculated through Eq. (24) for parallel-flow HE-NRs, where the hot and cool sides have the same working fluids and geometrical parameters.

$$P_{\text{NR}} = \frac{12\mu L}{H^3 W \rho^2 c_p^2}(C_1^2 + C_2^2) \tag{24}$$

From Fig. 1b, the flow rate on the hot fluid side of a HE-BER is equal to $(1 + R)$ times that of its referred HE-NR. Thus, when the hot and cool sides of a HE-BER have the same working fluids and geometrical parameters, the ratio of total pumping power with that of its referred HE-NR is calculated through Eq. (25).

$$\frac{P_{\text{BER}}}{P_{\text{NR}}} = \frac{1 + ((1+R)C_1/C_2)^2}{1 + (C_1/C_2)^2} \tag{25}$$

Compared with a HE-BER, the hot fluid flow rate of a HE-BIR is equal to $2R + 1$ times that of its referred HE-NR (see Fig. 1c). When the hot and cool sides have the same working fluids and geometrical parameters, the ratio of total pumping power between a HE-BIR and its referred HE-NR can be calculated through Eq. (26).

$$\frac{P_{\text{BIR}}}{P_{\text{NR}}} = \frac{1 + (1+2R)^2 C_1^2/C_2^2}{1 + (C_1/C_2)^2} \tag{26}$$

Similar to the above computation of K, a HE-RIR or HE-RER is divided into a small HE-NR and a small HE-BIR or HE-BER, and the total mechanical power consumption of a HE-RIR or HE-RER equals to the sum of power consumptions of small HE-NR and small HE-BIR or HE-BER. The pumping power of a small HE-NR is calculated

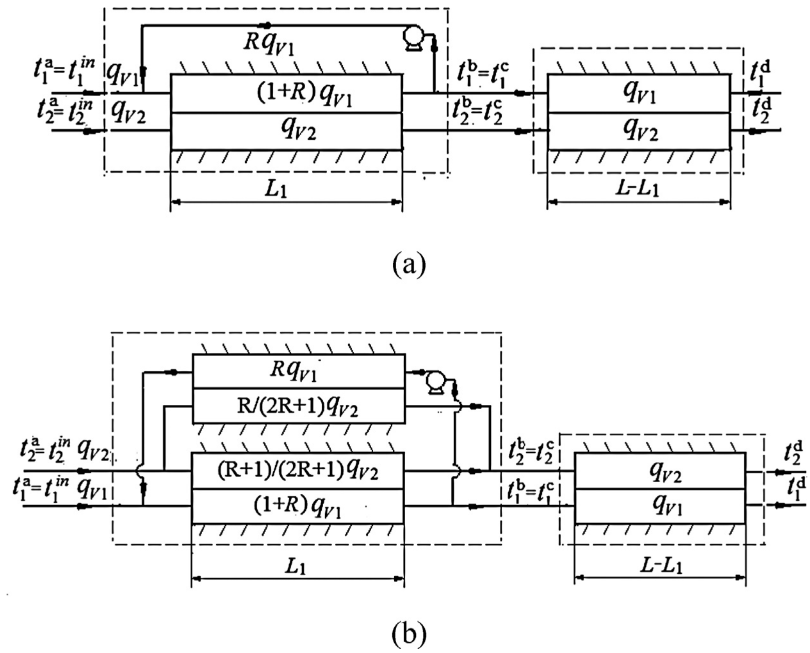

Fig. 2. Schematics of HE-RER and HE-RIR. (a) HE-RER and (b) HE-RIR.

through Eq. (24), while Eqs. (25) and (26) are adopted for the calculations of pumping powers of HE-BERs and HE-BIRs. Since the channel lengths of small HE-NR and HE-BER or HE-BIR are equal to L–L_1 and L_1, the total pumping powers for HE-RER and HE-RIR are calculated by Eqs. (27) and (28), respectively.

$$P_{\mathrm{RER}} = \frac{12\mu}{H^3 W \rho^2 {c_p}^2}((R^2+2R){C_1}^2 L_1 + (C_1^2 + C_2^2)L) \quad (27)$$

$$P_{\mathrm{RIR}} = \frac{12\mu}{H^3 W \rho^2 {c_p}^2} \cdot ((4R^2+4R){C_1}^2 L_1 + ({C_1}^2 + {C_2}^2)L) \quad (28)$$

3. Computation results and discussions

It is known from the theoretical model derived in Sections 2.1 and 2.3 that the thermo-hydraulic performances of heat exchangers with recycles can be constructed on the counterparts of heat exchangers without recycle, and the performances depend on quite a few factors, such as reflux ratio R, capacitance ratio C_1/C_2, heat transfer area A and recycle length L_1/L. For the conveniences to analyze the effects of recycles on the thermal augmentation, the dimensionless heat transfer rates, pumping power consumptions and overall performances (i.e., heat transfer rates under unit pumping power), which are normalized by the counterparts of reference heat exchangers with the same incoming flow rates, are adopted in the current work.

In order to investigate the effects of A on the heat transfer enhancement with recycles, four parallel-flow heat exchangers with no recycle (HE-NRs), whose geometrical parameters of hot sides are same as the counterparts on the cool fluid sides, are adopted as the reference heat exchangers in the current investigation. Moreover, the geometrical parameters of cross sections of the four reference exchangers are identical, while the passage lengths (L) are such set that their heat transfer areas equal to A_0, $0.35A_0$, $0.6A_0$, and $1.4A_0$. Furthermore, four different C_1/C_2 (=0.2, 0.3, 0.5 and 0.8) and L_1/L (=0.25, 0.5, 0.75 and 1.0) are adopted to investigate the effects of C_1/C_2 and L_1/L.

In the following computations it is assumed that the properties of working fluids are temperature-independent, and the flows on the hot and cool fluid sides are in the laminar flow regime. Furthermore, heat exchangers with recycles have the same working fluids, geometrical parameters and total heat transfer areas as those of the corresponding reference heat exchangers.

3.1. Heat exchangers with a basic external or internal recycle

Fig. 3a and b presents the variations of dimensionless heat transfer rate ($Q_{\mathrm{BER}}/Q_{\mathrm{NR}}$) with reflux ratio ($R$) for heat exchangers with basic external recycles (HE-BERs) under four different capacitance rate ratios (C_1/C_2) and heat transfer areas (A), respectively; while the variations of dimensionless heat transfer rate ($Q_{\mathrm{BIR}}/Q_{\mathrm{NR}}$) with reflux ratio ($R$) for heat exchangers with basic internal recycles (HE-BIRs) under different C_1/C_2 and A are presented in Fig. 4a and b, respectively. Furthermore, It is seen from Figs. 3 and 4 that both $Q_{\mathrm{BER}}/Q_{\mathrm{NR}}$ and $Q_{\mathrm{BIR}}/Q_{\mathrm{NR}}$ increase with the increment of R in most cases, and the maximum values under the combination of $C_1/C_2 = 0.8$ and $A = A_0$ are about 119% and 124% for HE-BERs and HE-BIRs, respectively (see Figs. 3a and 4a). Meanwhile, the maximum dimensionless heat transfer rates of about 121% and 127% are obtained in HE-BERs and HE-BIRs under the conditions of $C_1/C_2 = 0.2$ and $A = 0.35A_0$, respectively (see Figs. 3b and 4b), which is comparable to the counterpart of external recycle obtained in Ref. [22] (20.5%). Moreover, it is found that under the conditions of small R and small C_1/C_2 or large A, the values of $Q_{\mathrm{BER}}/Q_{\mathrm{NR}}$ and $Q_{\mathrm{BIR}}/Q_{\mathrm{NR}}$ are small and can be below unity, which indicates that improper R can result in the reduction of heat transfer rate compared with that of no recycle, in accordance with the conclusion obtained in Ref. [22]. Compared with external recycles, internal recycles can lead to larger decrements of heat transfer rate at small R, and a maximum reduction of about 2.4% is generated under the condition of $R = 0.3$, $C_1/C_2 = 0.2$ and $A = A_0$.

Figs. 3 and 4 also demonstrate that $Q_{\mathrm{BER}}/Q_{\mathrm{NR}}$ and $Q_{\mathrm{BIR}}/Q_{\mathrm{NR}}$ increase with the increment of C_1/C_2 and with the decrement of A for both HE-BERs and HE-BIRs. Under the cocurrent flow conditions of moderate R (=3), the maximums of $Q_{\mathrm{BIR}}/Q_{\mathrm{NR}}$ are equal to 118% and 119% for four different C_1/C_2 and A, respectively, while HE-BERs have the maximum dimensionless heat transfer rates of

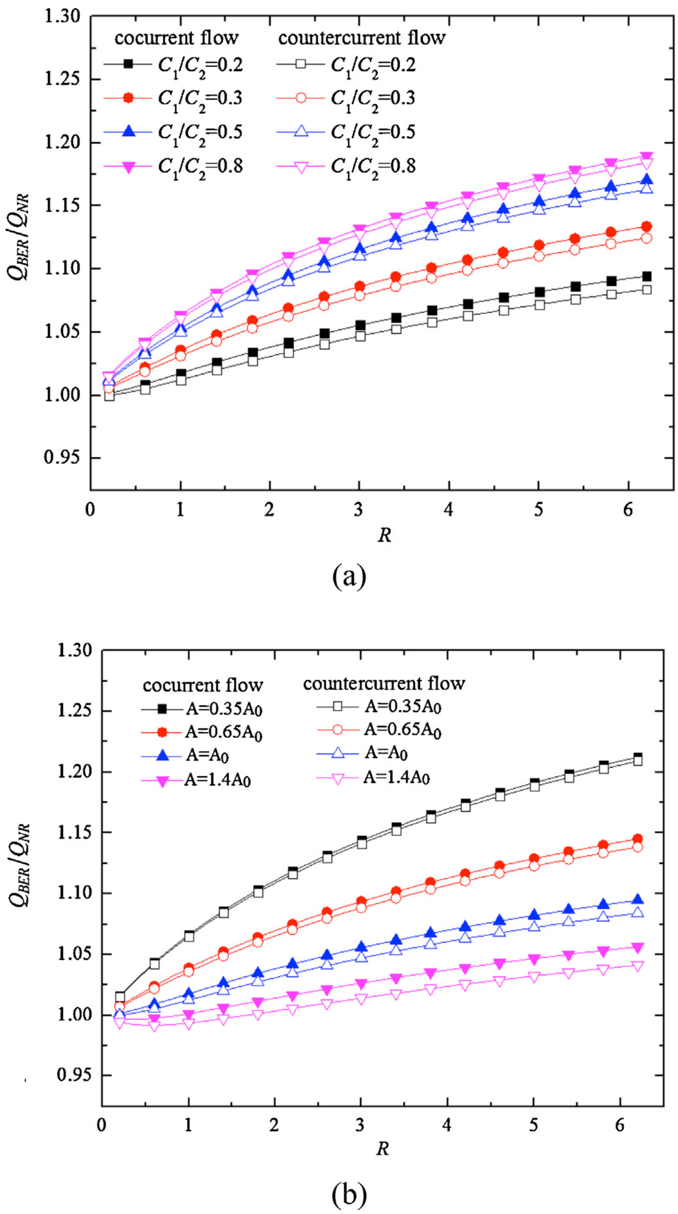

Fig. 3. Variations of ratio of Q between HE-BER and corresponding HE-NR (Q_{BER}/Q_{NR}) with R. (a) Variations of Q_{BER}/Q_{NR} under different C_1/C_2 when $A = A_0$ and (b) variations of Q_{BER}/Q_{NR} under different A when $C_1/C_2 = 0.2$.

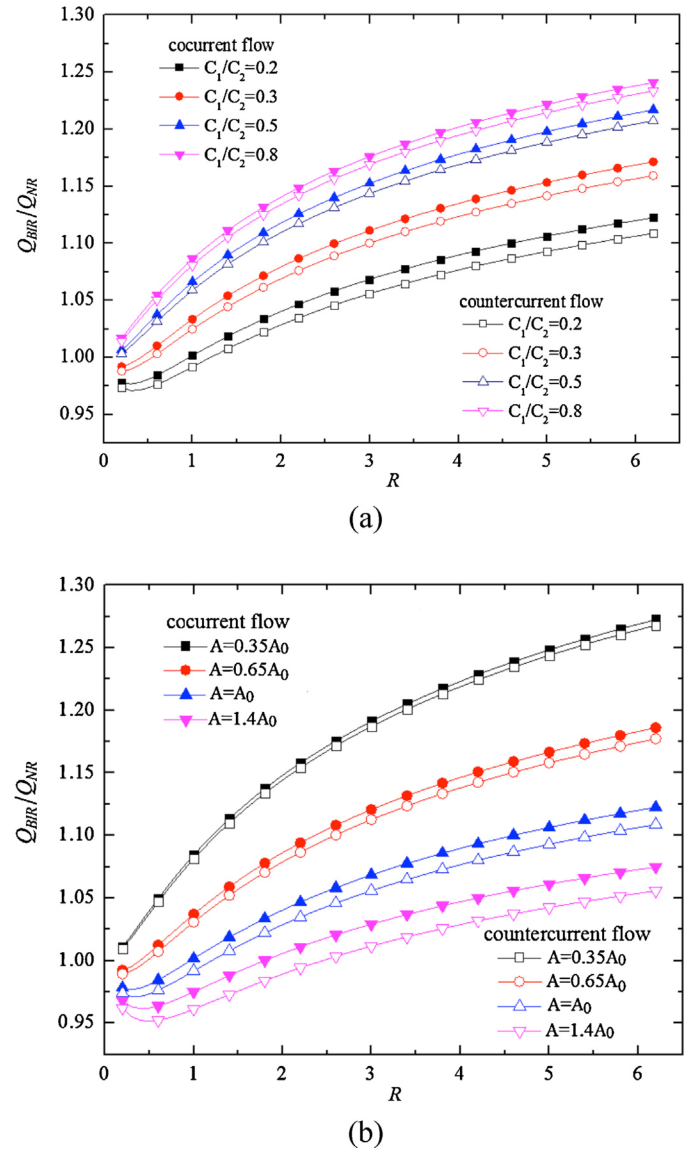

Fig. 4. Variations of ratio of Q between HE-BIR and corresponding HE-NR (Q_{BIR}/Q_{NR}) with R. (a) Variations of Q_{BIR}/Q_{NR} under different C_1/C_2 when $A = A_0$ and (b) Variations of Q_{BIR}/Q_{NR} under different A when $C_1/C_2 = 0.2$.

about 113.2% and 114.7% under four different C_1/C_2 and A, respectively. Compared with cocurrent flow conditions, countercurrent ones result in smaller Q_{BER}/Q_{NR} and Q_{BIR}/Q_{NR}, and the differences increase with the increment of A and the decrement of C_1/C_2.

Furthermore, by comparing HE-BERs with HE-BIRs (see Figs. 3 and 4) one can find that under the conditions of larger R, an internal recycle facilitates to generate good dimensionless heat transfer rate, while its dimensionless heat transfer rate is undesirable at small R conditions. As a contrast, HE-BERs have flatter slopes of Q_{BER}/Q_{NR} against R. Thus, external recycles can increase the heat transfer rates of heat exchangers more reliably.

To interpret the variations of dimensionless heat transfer rates of HE-BERs and HE-BIRs, we present the curves of dimensionless overall heat transfer coefficients (K_{BER}/K_{NR} and K_{BIR}/K_{NR}) and heat transfer temperature differences ($\Delta t_{m,BER}/\Delta t_{m,NR}$ and $\Delta t_{m,BIR}/\Delta t_{m,NR}$) with capacitance ratio (C_1/C_2) for discussions, as shown in Figs. 5 and 6. On the one hand, it is seen from Figs. 5a and 6a that both K_{BER}/K_{NR} and K_{BIR}/K_{NR} are larger than unity and increase with the increment of R and C_1/C_2, which indicates that the heat transfer rates of HE-BERs and HE-BIRs are larger than those of HE-NR, and increase with R and C_1/C_2 when heat transfer temperature differences keep constant. On the other hand, according to Eqs. (2) and (3), it is known that the discharge temperature on the hot fluid side decreases with the decrement of C_1/C_2. Therefore, the mixed inlet temperatures of HE-BERs and HE-BIRs (and thus $\Delta t_{m,BER}/\Delta t_{m,NR}$ and $\Delta t_{m,BIR}/\Delta t_{m,NR}$) decrease with the decreasing C_1/C_2 or increasing R (see Eqs. (8) and (13)), which is in accordance with what is depicted in Figs. 5b and 6b.

The heat transfer enhancements with recycles are determined by both K and Δt_m. When the increase of the former can compensate the decrease of the latter, a recycle can increase the heat transfer rate of heat exchanger, in accordance with what was concluded by Yeh [22]. Usually, the variation of the former with R overwhelms that of the latter, thus the heat transfer rate can be enhanced with a recycle in most cases. However, under the conditions of small R accompanied by small C_1/C_2 and large A, the discharge temperature on the hot fluid side is low, which results in remarkable drop of mixture temperature, while the increment

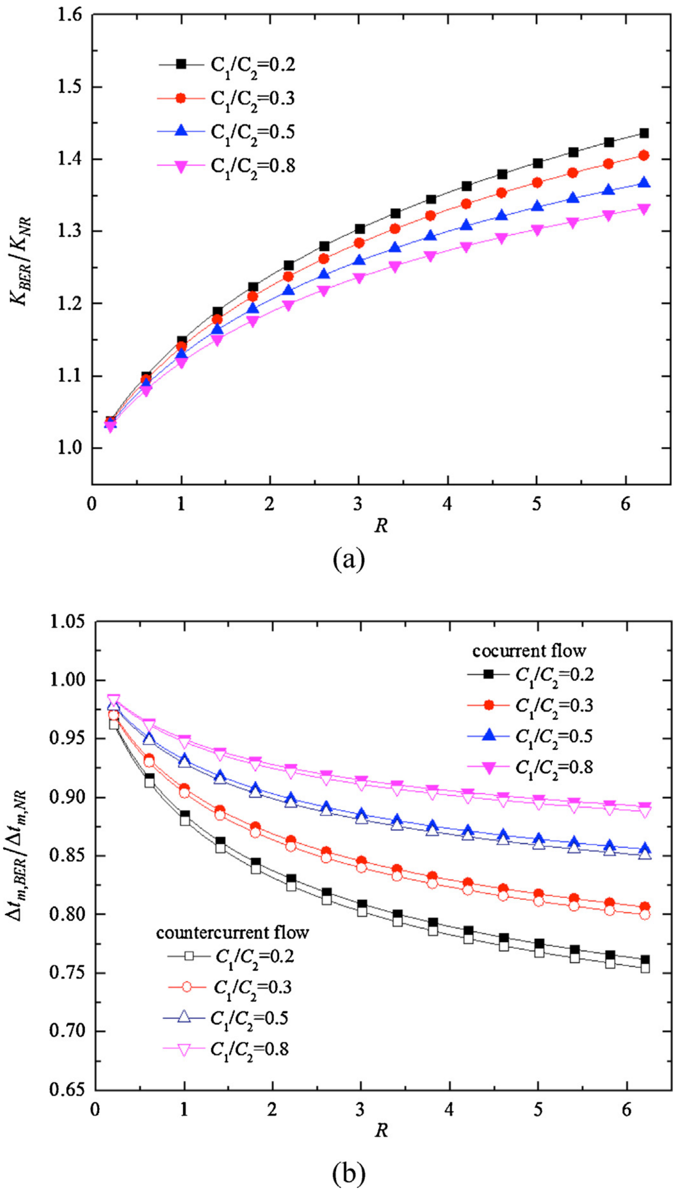

Fig. 5. Variations of ratios of K and Δt_m between HE-BER and corresponding HE-NR (K_{BER}/K_{NR} and $\Delta t_{m,BER}/\Delta t_{m,NR}$) with R under different C_1/C_2. (a) Variations of K_{BER}/K_{NR} and (b) Variations of $\Delta t_{m,BER}/\Delta t_{m,NR}$.

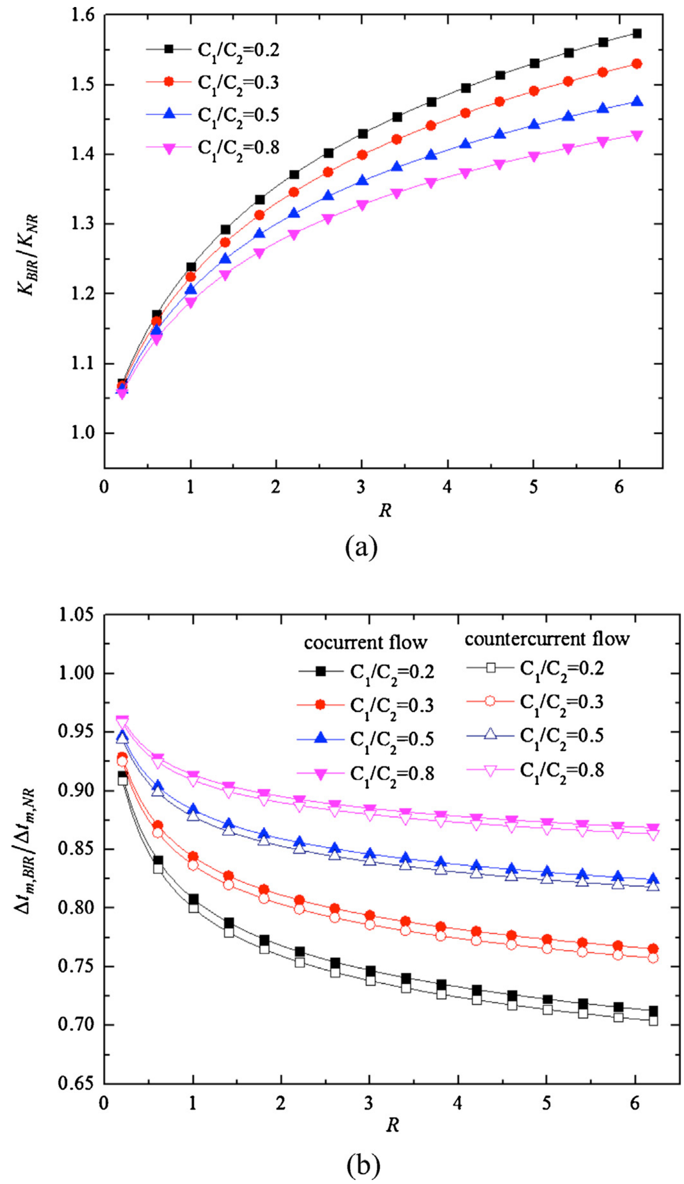

Fig. 6. Variations of ratios of K and Δt_m between HE-BIR and corresponding HE-NR (K_{BIR}/K_{NR} and $\Delta t_{m,BIR}/\Delta t_{m,NR}$) with R under different C_1/C_2. (a) Variations of K_{BIR}/K_{NR} and (b) Variations of $\Delta t_{m,BIR}/\Delta t_{m,NR}$.

of K is not that large under the same condition. Thereby, the heat transfer rate can be weakened, as shown in Figs. 3b and 4b.

It is also observed from Figs. 5 and 6 that compared with a HE-BER, a HE-BIR has a larger K under the same R, and the difference between them increases with the rising R. Meanwhile, the mixture temperature (and thus Δt_m) of HE-BIR is lower. Under larger R conditions, the increases of K dominate the variations of heat transfer rate. Thereby, a basic internal recycle can generate a larger heat transfer rate. On the contrary, Δt_m has more significant effect under smaller R conditions. Therefore, HE-BERs have some advantages at low reflux, which is in accordance with Figs. 3 and 4.

The variations of dimensionless pumping powers of HE-BERs and HE-BIRs, i.e., P_{BER}/P_{NR} and P_{BIR}/P_{NR} under four different values of C_1/C_2 are depicted in Fig. 7a and b, respectively. It is clear that P_{BER}/P_{NR} and P_{BIR}/P_{NR} exceed unity and they rise with the increment of R and C_1/C_2 at an increasing rate. Compared with HE-BERs, HE-BIRs require more pumping power under the same R and C_1/C_2. For an instance, under the conditions of moderate R (=3) and C_1/C_2 (=0.3), the pumping power consumptions of HE-BER and HE-BIR are increased to 2.24 and 4.96 times that of HE-NR, respectively.

The above researches are focused on the relative thermo-hydraulic performances of HE-BERs and HE-BIRs. To know more about the absolute variations of the heat exchanger performances induced by recycles, a numerical example is provided, where the incoming temperature difference between the hot and cool fluids was set to 40. The result indicates that the HE-NR achieve a heat transfer rate (Q) of 459 and require a pumping power (P) of 0.026 kW, while the Q and P of corresponding HE-BER and HE-BIR are equal to 511.9, 0.175 kW and 531.7, 0.5 kW, respectively. It is seen from these data that the P of HE-BER and HE-BIR are 6.7 and 19 times that of HE-NR, but the absolute variations are limited, i.e., an increment of 0.149 and 0.474 kW for HE-BER and HE-BIR, respectively. As a comparison, the relative variations of Q between HE-BER or HE-BIR and HE-NR is limited, while the absolute increment are notable, i.e., 52.9 and 72.7 kW for HE-BER and HE-BIR, respectively.

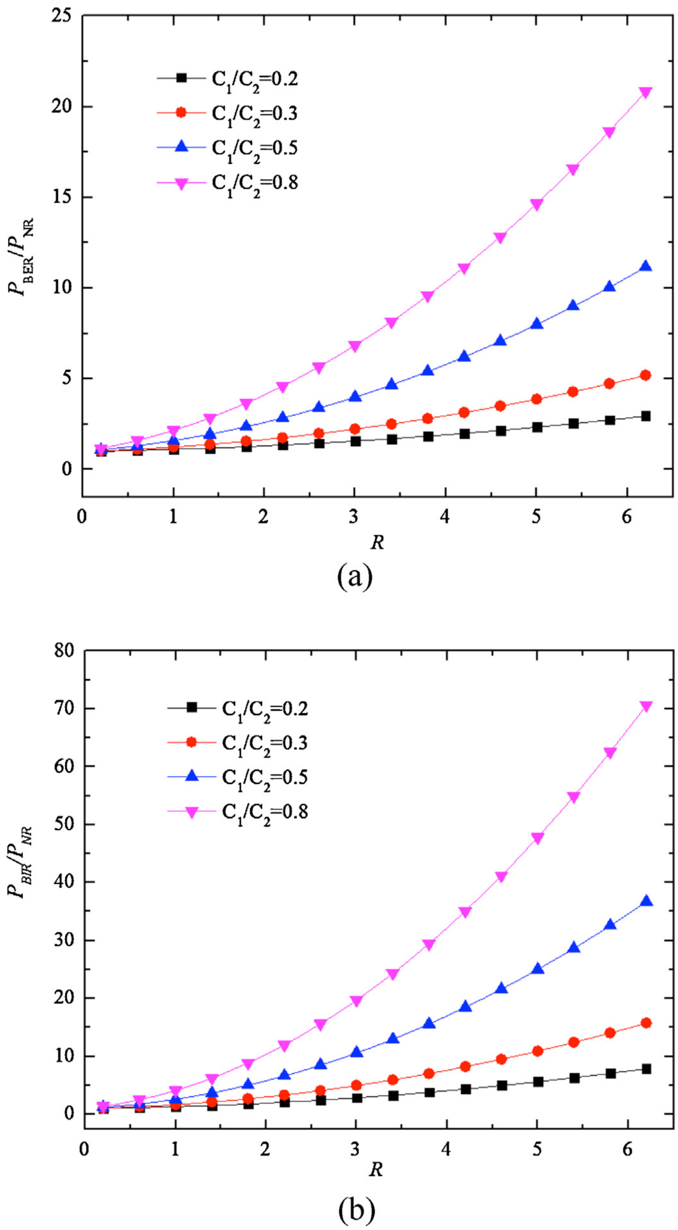

Fig. 7. Variations of ratios of P between HE-BER, HE-BIR and HE-NR (P_{BER}/P_{NR} and P_{BIR}/P_{NR}) with R under different C_1/C_2. (a) Variations of P_{BER}/P_{NR} and (b) Variations of P_{BIR}/P_{NR}.

These absolute changes demonstrate that the obtainment in heat transfer rate is much larger than the cost in the pumping power. This is because the flow is in the laminar regime which requires a relatively small pumping power. Therefore, it is reasonable to use the dimensionless quantities to evaluate the performance changes when recycles are adopted.

3.2. Heat exchangers with revised recycles

Fig. 8a–c presents the variations of dimensionless heat transfer rate (Q_{RER}/Q_{NR}), pumping power (P_{RER}/P_{NR}) and overall performance ($(Q/P)_{RER}/(Q/P)_{NR}$) with reflux ratio (R) for heat exchangers with revised external recycles (HE-RERs), respectively; and the counterparts of heat exchangers with revised internal recycles (HE-RIRs), i.e., Q_{RIR}/Q_{NR}, P_{RIR}/P_{NR} and $(Q/P)_{RIR}/(Q/P)_{NR}$ curves, are depicted in Fig. 9a–c, respectively. As mentioned above, in most cases except for small R, both Q_{BER}/Q_{NR} and Q_{BIR}/Q_{NR} exceed unity

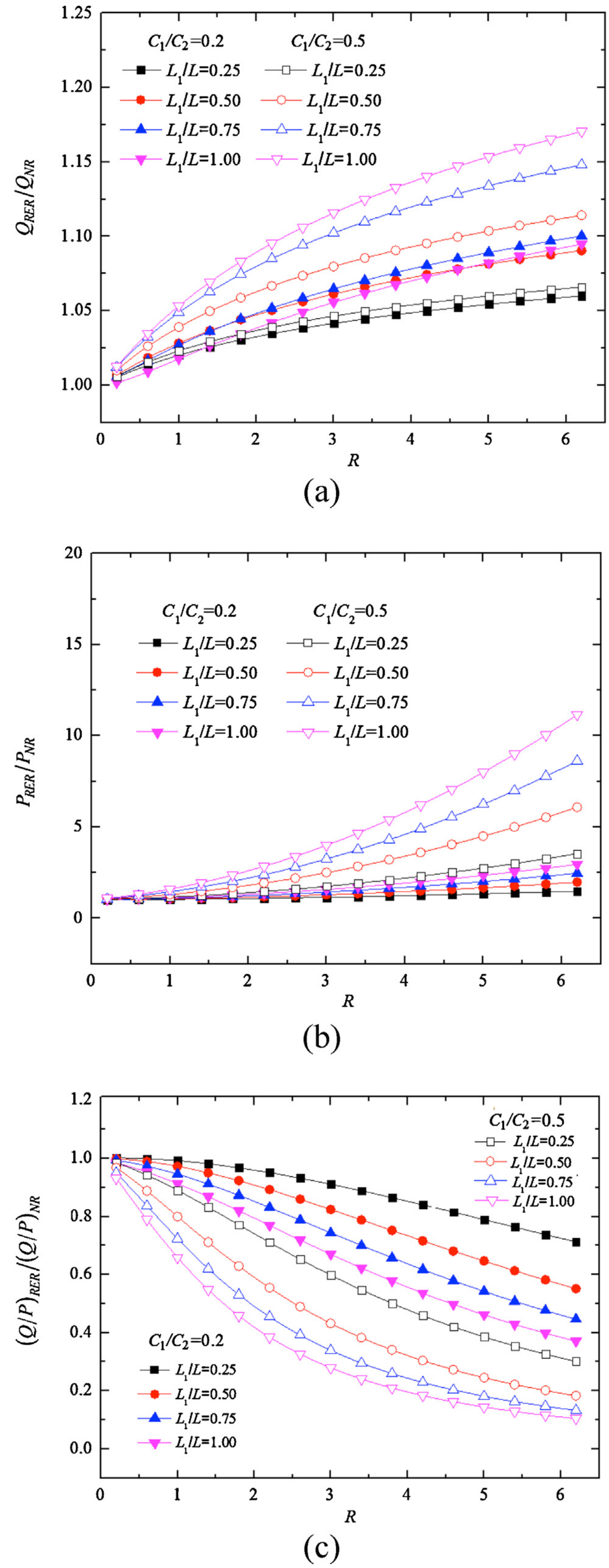

Fig. 8. Variations of ratios of thermo-hydraulic performances between HE-RER and HE-NR with R under difference recycle lengths (L_1/L) when $A = A_0$. (a) Variations of Q_{RER}/Q_{NR}; (b) Variations of P_{RER}/P_{NR}; and (c) Variations of $(Q/P)_{RER}/(Q/P)_{NR}$.

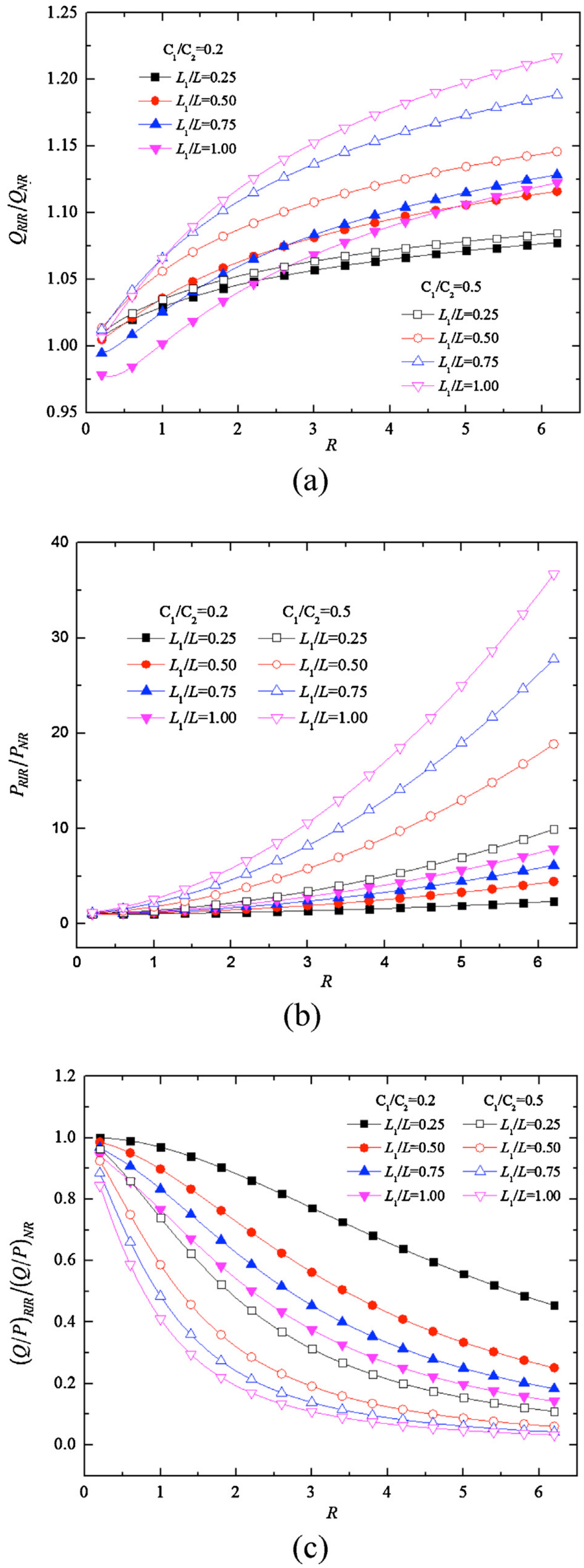

Fig. 9. Variations of ratios of thermo-hydraulic performances between HE-RIR and HE-NR with R under difference recycle lengths (L_1/L) when $A = A_0$. (a) Variations of Q_{RIR}/Q_{NR}; (b) Variations of P_{RIR}/P_{NR}; and (c) Variations of $(Q/P)_{RIR}/(Q/P)_{NR}$.

and rise with increasing R or capacitance rate ratio (C_1/C_2), and with decreasing heat transfer area (A). Thereby, Q_{RER}/Q_{NR} and Q_{RIR}/Q_{NR} also rise with the increment of R and C_1/C_2, while the variations of Q_{RER}/Q_{NR} and Q_{RIR}/Q_{NR} with recycle length (L_1/L) are complicated, as shown in Figs. 8a and 9a. The reason is that on the one hand a small HE-BER or HE-BIR in the system has a rising heat transfer area and thus a decreasing dimensionless heat transfer rate when L_1/L is increased (see Figs. 3b and 4b). However, the referred HE-NR with the same channel length of small HE-BER or HE-BIR (i.e., L_1) has an increasing heat transfer rate because its heat transfer area increases. On the other hand, when the recycle length of HE-RER or HE-RIR is increased, the small HE-NR (channel length L–L_1, see Fig. 2) decreases the heat transfer area, and its heat flux per area rises according to Eq. (19).

In the current investigation, it is found that under small R conditions, the decrement of L_1/L can result in a larger total heat transfer rate of HE-RER and HE-RIR, and Q_{RER}/Q_{NR} and Q_{RIR}/Q_{NR} exceed the counterparts of heat exchangers with a basic recycle. For an instance, when $R = 0.3$ and $C_1/C_2 = 0.2$, the heat transfer rate of HE-BIR is 97.6% of that of HE-NR, while the HE-RIR with $L_1/L = 0.25$ can obtain the heat transfer rate 1.1% larger than that of HE-NR under the same conditions of reflux ratio and capacitance rate ratio.

As mentioned above, the dimensionless pumping power of heat exchangers with basic recycles exceed unity and increase with R (see Fig. 7), thus, partial-length recycle can reduce the increment of pumping power effectively. It is seen from Figs. 8b and 9b that P_{RER}/P_{NR} and P_{RIR}/P_{NR} decrease with the decrements of R and L_1/L. For example, when $R = 3$, P_{RIR}/P_{NR} of quarter-length recycle under the conditions of $C_1/C_2 = 0.2$ and 0.5 are about 48% and 32% of the counterparts of HE-BIR, respectively, while the HE-RER with same recycle length has the decrement about 28% and 55% compared with that of HE-BER.

The dimensionless overall performances of HE-RERs and HE-RIRs, i.e., $(Q/P)_{RER}/(Q/P)_{NR}$ and $(Q/P)_{RIR}/(Q/P)_{NR}$ which can be calculated through Eqs. (17), (27) and (28), are depicted in Figs. 8c and 9c, respectively. It is seen from Figs. 8c and 9c that the dimensionless overall performances of HE-RERs and HE-RIRs are lower than unity, and the former has larger values. Moreover, it is observed in the two figures that both $(Q/P)_{RER}/(Q/P)_{NR}$ and $(Q/P)_{RIR}/(Q/P)_{NR}$ decrease with the increment of R and L_1, and smaller C_1/C_2 facilitates a better dimensionless overall performance. In more details, under the conditions of $R = 3$ and $C_1/C_2 = 0.2$, when L_1/L is decreased from 1 to 0.75, 0.5 and 0.25, $(Q/P)_{RER}/(Q/P)_{NR}$ increases by about 11%, 23% and 36%, respectively, while the increments under the combinations of $C_1/C_2 = 0.5$ and $R = 3$ are about 21.6%, 54.8% and 114.3% for the dimensionless recycle lengths of 0.75, 0.5 and 0.25, respectively. The effect of L_1/L on the dimensionless overall performance of a HE-BIR is similar to the counterpart of HE-RER, i.e., when L_1/L is decreased from 1 to 0.75, 0.5 and 0.25, the increments of $(Q/P)_{RIR}/(Q/P)_{NR}$ are about 21%, 49.8%, 105.6% and 27.5%, 75.7%, 187.7% for the above two capacitance rate ratios.

4. Conclusions

In the current work, parallel-flow heat exchangers with basic internal and external recycles, as well as revised recycles, are investigated in the laminar regime. Their theoretical models of thermo-hydraulic performances are constructed based on the counterparts of ordinary heat exchangers (i.e., with no recycle). Effects of reflux ratio (R), capacitance rate ratio (C_1/C_2), heat transfer area (A) and recycle length (L_1/L) on the dimensionless heat transfer rate (Q/Q_{NR}), pumping power (P/P_{NR}) and overall performance $(Q/P)/(Q/P)_{NR}$ of heat exchangers are studied.

Computation results demonstrate that the heat transfer rate of heat exchangers can be effectively enhanced by recycles in most cases, and Q/Q_{NR} of the basic external and internal recycles rises with the increase of R or C_1/C_2, or with the decrease of A. The maximum values of Q/Q_{NR} reach up to 121% and 127% for basic external and internal recycles, respectively. Moreover, it is shown that basic internal recycles result in larger dimensionless heat transfer rates under larger R conditions, while their dimensionless heat transfer performances are lower at smaller R. As a contrast, basic external recycles have more reliable performances over the whole R range. Furthermore, it is found that small R accompanied by small C_1/C_2 and large A results in a Q/Q_{NR} below unity, which indicates that the heat transfer rate can be weakened by an improper recycle.

The relation between Q/Q_{NR} and L_1/L is relatively complicated for the revised recycle. The dimensionless overall performances of heat exchangers with revised recycles are larger than the counterparts of corresponding basic recycled heat exchangers, because partial-length recycles results in smaller increments of pumping power. Under the condition of $R = 3$ and $C_1/C_2 = 0.5$, when L_1/L drops from 1 to 0.5, the values of $(Q/P)/(Q/P)_{NR}$ increase by 55% and 76% for revised external and internal recycles, respectively. Fluid recycling can increase heat transfer rates without changing geometrical structures and fluid flow rates, thus it is a competitive approach for heat transfer enhancement in heat exchangers.

Acknowledgments

This work was supported by the National Key Basic Research Development Program of China (2013CB228302) and the Natural Science Foundation of China (Nos. 51036003, 51076057).

References

[1] S.W. Qian, Handbook for Heat Exchanger Design, 1st ed., Chemical Industry Press, Beijing, 2002 (in Chinese).
[2] D.L. Gee, R.L. Webb, Forced convection heat transfer in helically rib-roughened tubes, Int. J. Heat Mass Transfer 23 (1980) 1127–1136.
[3] S.J. Eckels, T.M. Doerr, M.B. Pate, Heat transfer and pressure drop of R-134a and ester lubricant mixtures in a smooth and a micro-fin tube: part I – evaporation, ASHRAE Trans. 100 (1994) 265–281.
[4] K.M. Kim, B.S. Kim, D.H. Lee, H. Moon, H.H. Cho, Optimal design of transverse ribs in tubes for thermal performance enhancement, Energy 35 (2010) 2400–2406.
[5] S. Eiamsa-ard, C. Thianpong, P. Promvonge, Experimental investigation of heat transfer and flow friction in a circular tube fitted with regularly spaced twisted tape elements, Int. Commun. Heat Mass 33 (2006) 1225–1233.
[6] J. Guo, A.W. Fan, X.Y. Zhang, W. Liu, A numerical study on heat transfer and friction factor characteristics of laminar flow in a circular tube fitted with center-cleared twisted tape, Int. J. Therm. Sci. 50 (2011) 1263–1270.
[7] L. Wang, B. Sunden, Performance comparison of some tube inserts, Int. Commun. Heat Mass 29 (2002) 45–56.
[8] A.W. Fan, J.J. Deng, A. Nakayama, W. Liu, Parametric study on turbulent heat transfer and flow characteristics in a circular tube fitted with louvered strip inserts, Int. J. Heat Mass Transfer 55 (2012) 5205–5213.
[9] A.W. Fan, J.J. Deng, J. Guo, W. Liu, A numerical study on thermo-hydraulic characteristics of turbulent flow in a circular tube fitted with conical strip inserts, Appl. Therm. Eng. 31 (2011) 2819–2828.
[10] Y.H. You, A.W. Fan, W. Liu, S.Y. Huang, Thermo-hydraulic characteristics of laminar flow in an enhanced tube with conical strip inserts, Int. J. Therm. Sci 61 (2012) 28–37.
[11] K.J. Bell, Heat exchanger design for the process industries, J. Heat Transfer 126 (2004) 877–885.
[12] R. Mukherjee, Effectively design shell-and-tube heat exchanger, Chem. Eng. Prog. 94 (1998) 21–37.
[13] C.C. Gentry, Rodbaffle heat exchanger technology, Chem. Eng. Prog. 86 (1990) 48–57.
[14] J. Lutcha, J. Nemcansky, Performance improvement of tubular heat exchangers by helical baffles, Chem. Eng. Res. Des. 68 (1990) 263–270.
[15] Y.S. Wang, Z.C. Liu, S.Y. Huang, W. Liu, W.W. Li, Experimental investigation of shell-and-tube heat exchanger with a new type of baffles, Heat Mass Transfer 47 (2011) 833–839.
[16] Y.H. You, A.W. Fan, S.Y. Huang, W. Liu, Numerical modeling and experimental validation of heat transfer and flow resistance on the shell side of a shell-and-tube heat exchanger with flower baffles, Int. J. Heat Mass Transfer 25/26 (2012) 7561–7569.
[17] Y.H. You, A.W. Fan, X.J. Lai, W. Liu, S.Y. Huang, Experimental and numerical study of thermal-hydraulic performance of a shell-and-tube heat exchanger with trefoil-hole baffles, Appl. Therm. Eng. 50 (2013) 950–956.
[18] H.M. Yeh, S.W. Tsai, C.L. Chiang, Recycle effects on heat and mass transfer through a parallel-plate channel, AIChE J. 33 (1987) 1743–1746.
[19] C.D. Ho, H.M. Yeh, W.S. Sheu, An analytical study of heat and mass transfer through a parallel-plate channel with recycle, Int. J. Heat Mass Transfer 41 (1998) 2589–2599.
[20] H.M. Yeh, C.D. Ho, Solar air heaters with external recycle, Appl. Therm. Eng. 29 (2009) 1694–1701.
[21] H.M. Yeh, Y.Y. Peng, Y.K. Chen, Effect of external recycle on the performances of flat-plate solar air heaters with internal fins attached, Renew. Energy 34 (2009) 1340–1347.
[22] H.M. Yeh, Effect of external recycle on the performance in parallel-flow rectangular heat-exchangers, Tamkang J. Sci. Eng. 13 (2010) 405–412.
[23] J.P. Holman, Heat Transfer, 6th ed., McGraw-Hill, New York, 1986, pp. 526, 536, 545–547.
[24] R.B. Bird, W.E. Stewart, E.N. Lightfooe, Transport Phenomena, 2nd ed., Wiley & Son, New York, 2002, pp. 435.